Homoleptic gallium(III) and indium(III) aminoalkoxides as precursors for sol–gel routes to metal oxide nanomaterials†‡

Shashank Mishra,*[a] Stéphane Daniele,*[a] Sarah Petit,[a] Erwann Jeanneau[b] and Marc Rolland[c]

Received 27th October 2008, Accepted 14th January 2009
First published as an Advance Article on the web 13th February 2009
DOI: 10.1039/b818974a

New homoleptic aminoalkoxides of gallium(III) and indium(III) of the types $M_4\{(OC_2H_4)_2NMe\}_6$ [M = Ga (**1**), In (**2**)] and $[Ga\{(OC_2H_4)_3N\}]_n$ (**3**), as well as a previously described $Ga_2(OC_2H_4NMe_2)_6$ (**A**) have been prepared by isopropoxo(chloro)-aminoalkoxo exchange reactions and characterised by elemental analyses, FT-IR and ^{1}H NMR spectroscopy. Formation of a star-shaped $Ga[Ga\{\mu\text{-}\eta^3\text{:}\eta^1\text{-}(OC_2H_4)_2NMe\}_2]_3$ (**1**·4$CHCl_3$) and a zigzag linear $In_4\{\mu\text{-}\eta^3\text{:}\eta^1\text{-}(OC_2H_4)_2NMe\}_6$ (**2**·6$CHCl_3$), as revealed by X-ray single crystal structures, reflects the structural diversity among *N*-methyldiethanolaminate derivatives. Their hydrolyses in boiling water, either in presence or absence of tetraalkylamonium bromide, have been studied and, for gallium derivatives, compared with similar hydrolytic reactions of $Ga(O^iPr)_3$. The hydrolysed products were studied by FT-IR, TG-DTA and XRD techniques. For gallium derivatives, transition from orthorhombic Ga(O)OH phase of as-prepared powder to phase pure rhombohedral- and monoclinic-Ga_2O_3 occurred at about 500 °C and 700 °C, respectively, whereas cubic $In(OH)_3$ phase of as-prepared powder of **2** was converted to cubic In_2O_3 at 250 °C. Partial hydrolyses were also performed and evolution of the particle size in solution was recorded by light scattering measurements. Various sol–gel processing parameters such as concentration and hydrolysis ratio (h) were studied in order to stabilise nano-sized colloidal suspensions for access to thin films by spin coating. The *N*-methyldiethanolamine derivatives **1** and **2** were found to be the most suitable candidates for sol–gel processing. The transparent Ga_2O_3 and In_2O_3 films obtained on glass or Si wafers from spin-coating of **1** and **2**, respectively, were characterised by SEM, EDX and XRD.

Introduction

Mono- and multi-metallic oxides cover a wide range of electronic, optical and catalytic properties among which gallium- and indium-oxide have been the subjects of many investigations.[1,2] Gallium oxide (Ga_2O_3) is considered as one of the most ideal materials for application as thin-film gas sensors at high temperatures,[1] whereas indium oxide thin films are attractive materials to be used as transparent conductors in applications such as display panels and solar cell windows.[2] It is possible to switch the function of the gallium oxide sensor with temperature as this oxide has been shown to have a response to both reducing as well as oxidizing gases at about 500 and 900 °C, respectively.[3] On the other hand, un-doped indium oxide is used in industrial and technological applications such as toxic or dangerous gas detection in chemical plants due to its transparency and conductivity.[4] Indium oxide can be doped with other metal oxide to enhance its application in optics and electronics; for example, ZnO-In_2O_3 has gained attention as transparent and conductive oxide (TCO) films,[5] whereas SnO_2-In_2O_3 (ITO) has an optical band gap of more than 3.4 eV.[6] Besides above applications, these M_2O_3 (M = Ga, In) films also have other potential practical uses such as catalysts due to their high ion-exchange selectivity and capacity[7] and phosphor host materials for thin film electroluminescent (TFEL) devices.[8]

Access of the above materials has mainly been investigated by physical methods. Chemical routes to such materials, such as sol–gel (SG) processing, metal organic deposition (MOD) in the solution phase and chemical vapour deposition (CVD) in the vapour phase, require metallic precursors with suitable properties.[9] Among these routes, the sol-gel process is based on the hydrolysis and condensation of molecular precursors and offers many advantages such as processing at moderate temperature, lower cost and ease of fabrication of homogeneous, transparent, easily shaped, thermally and mechanically stable materials from a wide variety of precursors.[10] An understanding of the relationships between the properties of the materials and of their precursors is needed for the rational design of latter, which should thus be structurally well-characterised.[9] Metal derivatives of amino-alcohols are attractive precursors for the aforesaid chemical routes because of their solubility in a wide variety of organic solvents, favourable hydrolysis and condensation characteristics, good properties in terms of deposition (desired viscosity, rheology and stability of the

[a]*Université Lyon1, IRCELYON, 2 av. Albert Einstein, 69626 Villeurbanne, France. E-mail: mishrashashank74@rediffmail.com; Fax: +33 472 445 399; Tel: +33 472 445 329*
[b]*Université Lyon 1, Centre de Diffractométrie, 69622 Villeurbanne, France*
[c]*Université Montpellier II, IEM, CNRS-ENSCM, Place Eugène Bataillon, 34095 Montpellier, France*

† Electronic supplementary information (ESI) available: Variable temperature XRD patterns of powders obtained after hydrolysis of **3** (Fig. S1), IR and TG-DTA curves of as-prepared powder obtained after hydrolysis of $Ga(O^iPr)_3$ (Fig. S2 and S3), XRD of Ga_2O_3 film on glass obtained from **1** and calcined at 500 °C (Fig. S4), SEM images of Ga_2O_3 and In_2O_3 films on glass and Si surfaces (Fig. S5 and S6). CCDC reference numbers 704500 and 704501 for **1** and **2**, respectively. For ESI and crystallographic data in CIF or other electronic format see DOI: 10.1039/b818974a

‡ Dedicated to Prof. Anirudh Singh (University of Rajasthan, India) on the occasion of his 70th birthday.

solution), clean decomposition pathways and transformation into oxide at relatively low temperature, to name but a few.[11] Although a considerable literature is available on metal aminoalkoxides,[11] relatively few papers have been reported on aminoalkoxides of gallium and indium.[12] These publications, which mostly describe heteroleptic derivatives of the kind $R_xM(AA)_y$ (R = H, Me, Et, Cl; $x = y = 1$ or 2; M = Ga or In; AA = an aminoalcohol), are concerned with either structural and fundamental properties[13] or CVD experiments.[14] Only a handful reports are available on hydrolytic behaviour and deposition of metal oxide films *via* sol–gel processing of metal aminoalkoxides as a general class,[15] none of these being concerned with gallium or indium aminoalkoxides.

In this paper, we wish to report synthesis and characterisation of homoleptic gallium(III) and indium(III) aminoalkoxide precursors based on *N*-methyl substituted aminoethanol, namely *N*, *N*-dimethylethanolamine (dmeaH), *N*-methyldiethanolamine ($mdeaH_2$) and triethanolamine ($teaH_3$). These well-characterised derivatives were investigated for different sol–gel parameters and employed for the elaboration of Ga_2O_3 and In_2O_3 nanoparticles as well as films by spin-coating.

Results and discussion

(a) Synthesis and spectroscopic properties

New gallium(III) aminoalkoxides **1** and **3** were synthesised by isopropoxo-aminoalkoxo exchange reactions using $Ga(O^iPr)_3$ and either *N*-methyldiethanolamine or triethanolamine as starting reagents in toluene, whereas indium(III) derivative **2** was prepared by a metathesis reaction of anhydrous $InCl_3$ and sodium salt of *N*-methyldiethanolamine in THF (Scheme 1). For indium derivative, it was essential to reflux the reaction mixture for few hours in order to avoid the formation of an heteroleptic complex of the composition $[InCl(mdea)]_n$. The complex $Ga_2(OC_2H_4NMe_2)_6$, which has been synthesised previously from the reaction of $Ga(NR_2)_3$ (R = Me, Et, $SiMe_3$) and *N*, *N*-dimethylethanolamine (dmeaH) in toluene or ether and characterised spectroscopically,[14e,15f] was also synthesised by the alcoholysis reaction of $Ga(O^iPr)_3$ with dmeaH in toluene in order to compare its hydrolytic reactions and deposition properties with new gallium aminoalkoxides **1** and **3**. Unlike solid derivatives **2** and **3**, the freshly prepared **1** is a viscous mass but gives colourless crystalline solid on crystallisation from chloroform. All the derivatives show good solubility in THF, diethyl ether, toluene and alcohols.

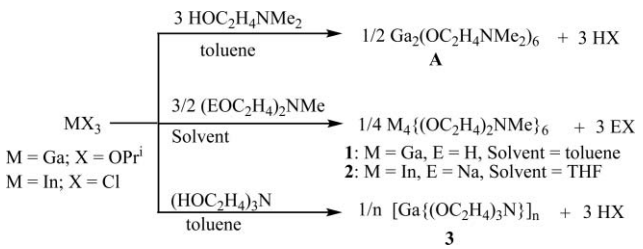

Scheme 1 Synthesis of derivatives **A** and **1–3**.

Compared to parent aminoalcohols, IR spectra of the new compounds **1–3** show two new features: (i) absence of absorption bands due to ν(OH) in the region 3100–3500 cm^{-1}, thus confirming absence of species solvated by the parent aminoalcohol, and (ii) appearance of new bands in the region 665–419 cm^{-1} for νM–O and νM–N stretching. The room temperature ^{1}H NMR spectra of new derivatives **1–3** are simple and show that these compounds are fluxional under these conditions. The protons of ethylene group(s) form an AA′BB′ spin system and appear either as two distinct triplets (complex **2**) or relatively broad signals with some evidence of splitting (complex **A**, **1** and **3**) in the region δ 2.75–2.80 and 3.72–3.80 ppm for NCH_2 and OCH_2 groups, respectively. The protons of methyl group(s) on nitrogen atom in **A**, **1** and **2** are observed as a singlet at δ 2.48–2.50 ppm. The above fluxional behaviour can be checked by lowering measurement temperature. For example, in the variable temperature ^{1}H NMR spectra of **1**, the broad peaks observed for ethylene moiety at room temperature start becoming sharper with well-defined multiplicities on lowering temperature and the spectrum recorded at 233 K shows two distinct triplets and a multiplet for OCH_2 and NCH_2 protons, respectively (Fig. 1).

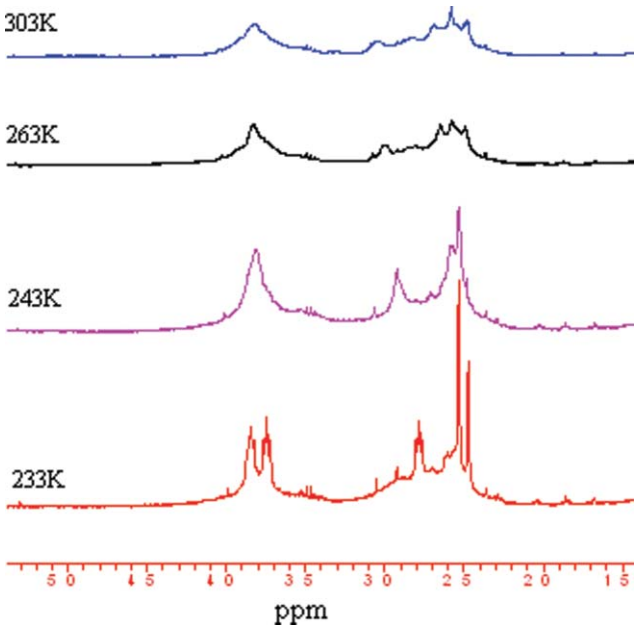

Fig. 1 Variable temperature ^{1}H NMR spectra of **1** in $CDCl_3$.

(b) Molecular structures of 1 and 2

The star-shaped structure of $Ga_4\{(OC_2H_4)_2NMe\}_6$ (**1**·4$CHCl_3$) can be assumed as a central Ga^{3+} cation being coordinated with three peripheral bis-(*N*-methyldiethanolamino)gallate $[Ga\{(\mu\text{-}OC_2H_4)(OC_2H_4)NMe\}_2]^-$ units, which act as a bidentate chelating ligand through two oxygen atoms (Fig. 2). All the four gallium atoms are six-coordinate with an all-oxygen environment O_6 for the central gallium atom and a mixed oxygen–nitrogen N_2O_4 environment for three peripheral gallium atoms, the former having more regular octahedral geometry than the latter. As expected, the terminal Ga–O bond distances are shorter (av. 1.88 Å) than the bridging Ga–O ones (av. 1.95 Å) (Table 1). The Ga–N distances, spreading in the range 2.258(4)–2.305(3) Å, are considerably longer than those found in $[GaH\{(\mu\text{-}OC_2H_4)(OC_2H_4)NMe\}_2]_2$ (av. 1.192 Å).[13g] All four gallium ions are located in a plane, with Ga–Ga–Ga angles of about 120°. The central gallium is equally distant with three peripheral gallium atoms, the distance

Table 1 Selected bond length and angles for **1**

Bond lengths/Å			
Ga1–O1	1.945(3)	Ga2–O1^a	1.968(3)
Ga1–O3	1.951(3)	Ga2–O2^a	1.870(3)
Ga1–O4	1.962(2)	Ga2–N1^a	2.258(4)
Ga1–O1^a	1.945(3)	Ga3–O3	1.954(2)
Ga1–O3^a	1.951(3)	Ga3–O4	1.955(3)
Ga1–O4^a	1.962(2)	Ga3–O5	1.874(3)
Ga2–O1	1.968(3)	Ga3–O6	1.883(3)
Ga2–O2	1.870(3)	Ga3–N3	2.295(3)
Ga2–N1	2.258(4)	Ga3–N3^a	2.305(3)
Bond angles/°			
O1–Ga1–O3	164.4(1)	O1^a–Ga2–O2	99.3(1)
O1–Ga1–O4	95.8(1)	O2–Ga2–O2^a	145.9(1)
O1–Ga1–O1^a	75.0(1)	O2–Ga2–N1^a	85.4(1)
O1–Ga1–O3^a	94.2(1)	N1–Ga2–N1^a	132.9(1)
O1–Ga1–O4^a	98.6(1)	O1^a–Ga2–O2^a	107.9(1)
O3–Ga1–O4	74.4(1)	O1^a–Ga2–N1^a	77.0(1)
O1^a–Ga1–O3	94.2(1)	O2^a–Ga2–N1^a	81.1(1)
O3–Ga1–O3^a	98.5(1)	O3–Ga3–O4	74.5(1)
O3–Ga1–O4^a	93.6(1)	O3–Ga3–O5	97.7(1)
O1^a–Ga1–O4	98.6(1)	O3–Ga3–O6	111.0(1)
O3^a–Ga1–O4	93.6(1)	O3–Ga3–N3	77.0(1)
O4–Ga1–O4^a	161.9(1)	O4–Ga3–O5	112.0(1)
O1^a–Ga1–O3^a	164.4(1)	O4–Ga3–O6	97.4(1)
O1^a–Ga1–O4^a	95.8(1)	O4–Ga3–N3	148.5(1)
O3^a–Ga1–O4^a	74.4(1)	O5–Ga3–O6	143.5(1)
O1–Ga2–O2	107.9(1)	O5–Ga3–N3	84.9(1)
O1–Ga2–N1	77.0(1)	O6–Ga3–N3	80.4(1)
O1–Ga2–O1^a	74.0(1)	Ga1–O1–Ga2	105.5(2)
O1–Ga2–O2^a	99.3(1)	Ga1–O3–Ga3	105.8(1)
O1–Ga2–N1^a	149.6(1)	Ga1–O4–Ga3	105.3(1)
O2–Ga2–N1	81.1(1)		

^{a} Symmetry code: $-x$, y, $1/2 - z$.

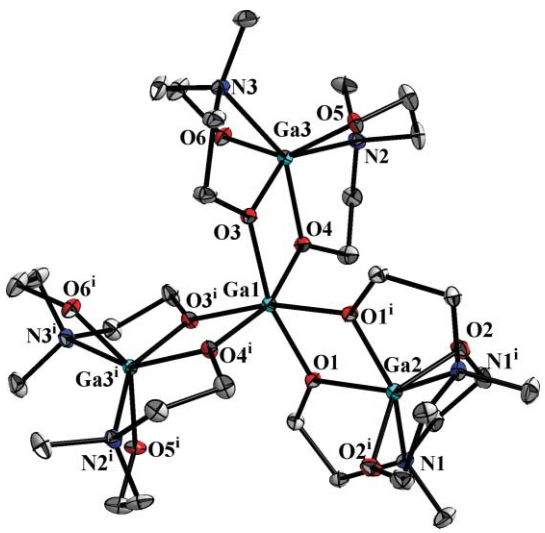

Fig. 2 Molecular structure of **1** with ellipsoids at 30% probability. Hydrogen atoms have been omitted for clarity. Symmetry codes: (i) $-x$, y, $1/2 - z$.

3.113(6) being slightly longer than those found in other start-shaped tetranuclear gallium derivatives, for example in Ga[Ga(μ-O^{i}Pr)$_2$(O^{i}Pr)$_2$]$_3$ (av. 3.013 Å).[16] The planar Ga_2O_2 rings have inner ring angles of almost 75° and 105° for gallium and bridging oxygen atoms, respectively. These star-shaped tetranuclear units are well separated by solvated $CHCl_3$ molecules with no significant interactions between either two Ga_4 units or a Ga_4 unit and solvated chloroform molecules. The structure of **1** can be related to the 'Mitsubishi' type of structure described for trivalent aluminium and lanthanide metals.[17]

In contrast to **1**, the indium analogue $In_4\{(OC_2H_4)_2NMe\}_6$ (**2**·6$CHCl_3$) has a zigzag linear structure, which can be described as a central $[In_2\{(\mu\text{-}OC_2H_4)(OC_2H_4)NMe\}_2]^{2+}$ cation being coordinated with two peripheral metallate $[In\{(\mu\text{-}OC_2H_4)(OC_2H_4)NMe\}_2]^-$ units (Fig. 3). All the four indium atoms are six-coordinate with NO_5 environment for the indium atoms in central $[In_2\{(\mu\text{-}OC_2H_4)(OC_2H_4)NMe\}_2]^{2+}$ moiety and a N_2O_4 environment for two peripheral $[In\{(\mu\text{-}OC_2H_4)(OC_2H_4)NMe\}_2]^-$ units. The geometry around four indium atoms can be considered as highly distorted octahedral. As expected, the average terminal In–O bond distance, 2.064 Å, is slightly shorter than the average bridging In–O one, 2.144 Å (Table 2). The In–N distances, which are found in the rage 2.325(4)–2.424(3) Å, compare well with those reported for some other indium aminoalkoxides having terminal In–N bonds[13e,14f] but are considerably shorter than the distances 2.516(2)–2.930(2) Å found in dimeric complexes $[Me_2In(OR)]_2$ [R = $CH_2CH_2NMe_2$, $CH(Me)CH_2NMe_2$ or $CH(CHNMe_2)_2$].[14c] The distance between two central In1–In1^i [3.405(5)] is slightly shorter than 3.465(4) Å found between central-peripheral metals *i.e.* In1–In2. The three planar In_2O_2 rings have inner ring angles of 71.3(1)–74.4(1)° and 105.5(1)–108.2(1)° for indium and bridging oxygen atoms, respectively. As found for gallium analogue **1**, there are no significant interactions between either two In_4 units or In_4 unit and solvated chloroform molecules.

Our efforts to get X-ray quality crystals of the **3** were unsuccessful, which precluded solid-state structural determination of

Table 2 Selected bond length and angles for **2**

Bond lengths/Å			
In1–O1	2.127(3)	In2–O2	2.068(3)
In1–O4	2.152(3)	In2–O3	2.061(3)
In1–O5	2.117(3)	In2–O4	2.164(3)
In1–O6	2.083(3)	In2–N1	2.424(3)
In1^a–O5	2.158(3)	In2–N2	2.375(3)
In2–O1	2.150(3)	In1–N3	2.325(4)
Bond angle/°			
N3–In1–O5^a	76.6(1)	N1–In2–N2	142.3(1)
N3–In1–O1	109.3(1)	N1–In2–O1	73.6(1)
O5^a–In1–O1	162.5(1)	N2–In2–O1	143.0(1)
N3–In1–O5	149.1(1)	N1–In2–O2	77.8(1)
O5^a–In1–O5	74.4(1)	N2–In2–O2	88.8(1)
O1–In1–O5	101.5(1)	O1–In2–O2	114.2(1)
N3–In1–O6	79.1(1)	N1–In2–O3	87.2(1)
O5^a–In1–O6	105.6(1)	N2–In2–O3	77.7(1)
O1–In1–O6	91.8(1)	O1–In2–O3	101.3(1)
O5–In1–O6	98.4(1)	O2–In2–O3	134.9(1)
N3–In1–O4	91.0(1)	N1–In2–O4	141.9(1)
O5^a–In1–O4	91.6(1)	N2–In2–O4	75.3(1)
O1–In1–O4	72.1(1)	O1–In2–O4	71.4(1)
O5–In1–O4	100.3(1)	O2–In2–O4	103.6(1)
O6–In1–O4	157.4(1)	O3–In2–O4	113.8(1)

^{a} Symmetry codes: $2 - x$, $2 - y$, $1 - z$.

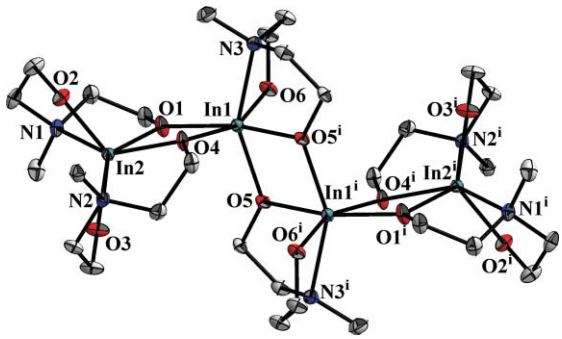

Fig. 3 Molecular structure of **2** with ellipsoids at 30% probability. Hydrogen atoms have been omitted for clarity. Symmetry codes: (i) $2-x, 2-y, 1-z$.

this compound. It is worth mentioning here that the aluminium analogue of **3** has a star-shaped tetra-nuclear structure $[Al(tea)]_4$ both in solid- and solution-state, as shown by single crystal structural study and variable temperature NMR experiments, respectively.[18]

(c) Hydrolyses

Complete hydrolyses of the derivatives **1–3** and **A** were performed in boiling water and the resulting powders obtained were separated by centrifugation and, after washing with water and ethanol, characterised by FT-IR, TG-DTA as well as XRD at variable temperatures. The XRD patterns of the powders obtained from the hydrolysis of gallium derivatives **A**, **1** and **3** and annealed at different temperatures were similar. Fig. 4 shows the variable temperature XRD patterns for **1**, whereas similar patterns for derivative **3** are shown in ESI (Fig. S1).† These figures show the formation of crystallised, phase pure orthorhombic Ga(O)OH (JCPDS no. 54-0910) for the as-prepared powders. The presence of hydroxyl group and some remaining organic residues is indicated by FT-IR spectra of these as-prepared powders (Fig. 5), the latter could be eliminated on calcinations below 400 °C, as shown by TGA and DTA curves in Fig. 6 and Fig. 7, respectively. The TG-DTA curves of hydrolysed powders obtained from gallium derivatives show a 2-step decomposition process with an endothermic peak at 100 °C and an exothermic peak at about 300 °C due to loss of adsorbed solvent or water and pyrolysis of residual organics, respectively. The crystallised orthorhombic GaO(OH) phase of as-prepared powders first turned amorphous on calcination at 200 °C and

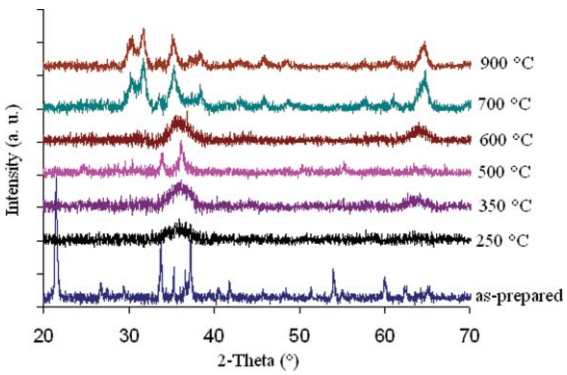

Fig. 4 Variable temperature XRD patterns of the powder obtained after hydrolysis of **1**.

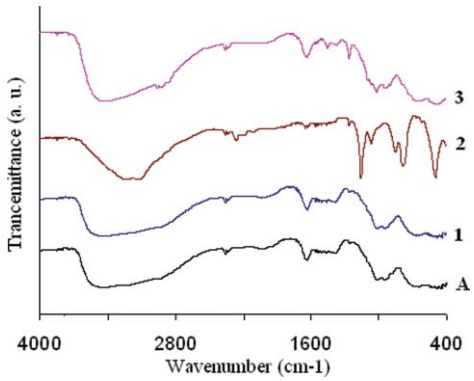

Fig. 5 FT-IR spectra of the as-prepared samples obtained after hydrolyses of **1–3** and **A**.

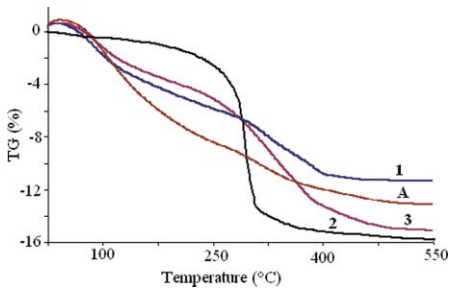

Fig. 6 TGA curves of the as-prepared samples obtained after hydrolyses of **1–3** and **A**.

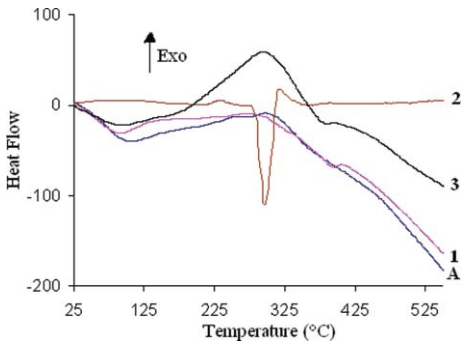

Fig. 7 DTA curves of the as-prepared samples obtained after hydrolyses of **1–3** and **A**.

then started converting to Ga_2O_3 at about 250 °C. The XRD of the samples annealed at 500 °C exhibited a phase pure rhombohedral Ga_2O_3 (JCPDS no. 01-074-1610). Rhombohedral Ga_2O_3, in bulk, form at about 500 °C has previously been observed by other workers.[19] Transition from rhombohedral phase to monoclinic one (JCPDS no. 041-1103) occurred at 700 °C. Hydrolyses of the derivatives **1–3** and **A** were also performed in the presence of *tert*-butyl ammonium bromide in boiling water. Previous work from this laboratory has shown the use of ammonium bromide salts as additives in the sol-gel synthesis of porous, highly crystalline TiO_2 nanoparticles at low temperature.[20] However, its presence has little influence on the hydrolytic behaviour of **1–3** and **A** (Fig. S1).† For the sake of comparison, hydrolysis of $Ga(O^iPr)_3$ under similar conditions was also studied and the FT-IR spectrum and TG-DTA curves of as-prepared powder obtained are shown in ESI (Fig. S2 and S3).† The TG-DTA curves exhibit a

single-step decomposition process with a strong endothermic peak at 420 °C. The variable temperature XRD patterns (shown in Fig. 8) indicate that transitional behaviour, from orthorhombic GaO(OH) to rhombohedral Ga_2O_3 and then to monoclinic Ga_2O_3, is similar to those obtained from gallium aminoalkoxides **A**, **1** and **3**. However, particles are much smaller for gallium aminoalkoxides as illustrated by broad peaks in their diffraction patterns (Fig. 4, S1).† The size of the orthorhombic GaO(OH) and monoclinic Ga_2O_3 particles obtained from gallium aminoalkoxides were calculated by the Debye–Scherrer formula to be in the range 25–40 and 13–17 nm, respectively, as against 40–50 and 20–25 nm for similar phases obtained from $Ga(O^iPr)_3$. This difference in particle size may be explained by the much better complexation and stabilisation by chelating aminoalkoxide ligands as compared to isopropoxide.

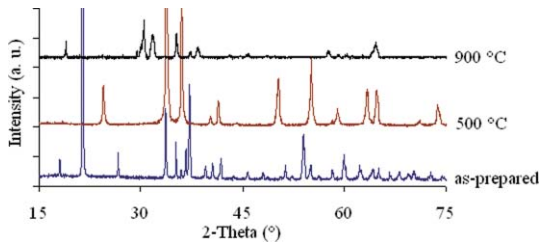

Fig. 8 Variable temperature XRD patterns of powder obtained after hydrolysis of $Ga(O^iPr)_3$.

In contrast to gallium aminoalkoxides **A**, **1** and **3**, the as-prepared powder from the indium derivative **2** showed that it is crystallised cubic $In(OH)_3$ (JCPDS no. 04-008-9898) (Fig. 9). The TGA curve for this as-prepared powder exhibits single step decomposition in the temperature range 210–320 °C (Fig. 6), the DTA curve in Fig. 7 showing a strong endothermic peak at 295 °C. This is in contrast to gallium analogue **1**, where remaining organic residues were present till 400 °C. The $In(OH)_3$ phase is converted to cubic In_2O_3 (JCPDS no. 006-0416) at temperature as low as 250 °C (Fig. 9). This temperature is about 100 °C lower than for In_2O_3 obtained from the hydrolysis of $In(OEt)_3$.[2a] The size of the $In(OH)_3$ and In_2O_3 particles, estimated from the Debye–Scherrer formula, were in the range 24–32 and 15–17 nm, respectively.

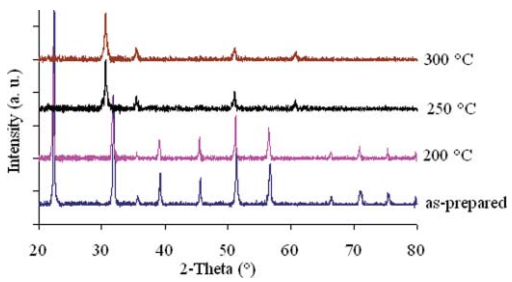

Fig. 9 Variable temperature XRD patterns of powder obtained after hydrolysis of **2**.

Table 3 Average particle sizes for the partially hydrolysed **A** and **1–3** in isopropanol

Precursor	Conc./ ML^{-1}	Hydrolysis ratio (h)	Average particle size/nm	Observation on hydrolysed product
A	0.054	2	148	Clear sol, stable up to 3–4 d
	0.054	4	1427	Thin gel formation within 1–2 h, reversible on shaking
	0.054	5	1437	Thin gel formation within 1–2 h, reversible on shaking
	0.054	6	1978	Viscous gel formation within 1 h, reversible on shaking
	0.054	8	Over 3000	Precipitation in a few h
1	0.065	2	243	Clear sol, stable for more than 7 d
	0.065	4	284	Clear sol, stable for more than 7 d
	0.065	5	349	Clear sol, stable for 5–6 d
	0.065	6	599	Clear sol, stable for 5–6 d
	0.065	8	780	Clear sol, stable for 3–4 d
	0.78	4	1974	Gel formation within 1–2 h, reversible on shaking
2	0.070	2	300	Sol, stable for 2–3 d
	0.070	4	370	Sol, stable for 2–3 d
	0.070	5	450	Sol, stable for 1 d
	0.070	6	561	Sol, stable for 1 d
	0.30	4	422	Sol, stable for 2 d
3	0.087	2	1914	Immediate gel formation
	0.087	4	2688	Precipitation in 1–2 h
	0.087	5	2819	Precipitation in 1–2 h
	0.087	6	Over 3000	Precipitation in 1 h

(d) Preparation of colloidal suspensions and particle size determination

Colloidal suspensions or gelatinous media are usually required for the elaboration of thin films *via* solution routes. The stability of the colloidal media is also of importance for industrial applications, hence, partial hydrolysis and aging phenomena were investigated. Partial hydrolyses of **1–3** and **A** were performed by mixing 0.05–0.8 M solutions in isopropanol with a 0.2–0.8 M solutions of water in the same solvent, to achieve $h = 2$, 4, 5, 6 or 8. Hydrolysed solutions were stored under argon for few hours at room temperature and evolution of the particle size in solution was recorded by light scattering measurements. The behaviour of precursors **1–3** and **A** were different for different hydrolysis ratio (h) (Table 3). For 0.05 M solutions of the gallium compound **1**, sols stable up to 4–7 d were obtained for $h = 2$, 4, 5, 6 and 8 with average particle size increasing gradually from 243–780 nm. The increase in concentration up to 0.78 M led to formation of gel of about 2000 nm particle size. The sols obtained from the

partial hydrolysis of indium analogue **2** were relatively less stable (up to 2 or 3 d) with particle size varying in the range 300–750 nm for h = 2–6 (conc. = 0.065 or 0.78 M). In contrast, only h = 2 gave sol for **A**, which was stable up to 3–4 d. Solutions with higher hydrolysis ratios were difficult to handle and had poor stability, forming either thin gels (h = 4 and 5) or viscous gels within 1–2 h. These gels were reversible by shaking, giving sols of large particles (about 1500–2000 nm). For $h \sim 8$, precipitation was observed after a few hours (particle sizes larger than 2500 nm). On the other hand, either a gel formation (h = 2) or a precipitations (h = 4–6) was observed for triethanolamine derivative **3**, with particle size varying from 1900 to over 3000 nm. These results indicate that the *N*-methyldiethanolamine derivatives **1** and **2** are best candidates among the complexes reported here for spin coatings.

(e) Elaboration and characterisation of the films

Following above observations, the *N*-methyldiethanolamine derivatives **1** and **2** were used to elaborate Ga_2O_3 and In_2O_3 films, respectively, by spin coating. Keeping in mind the viability of *in situ* reactions, isopropanol and chloroform were taken as solvent for **1** and **2**, respectively. 0.1 mL of sols obtained by hydrolysis of solution of **1** and **2** (conc. = 0.3–0.7 M, h = 2) were dropped rapidly on the pre-cleaned glass or Si substrate, spinning at a speed of 1200–2000 rpm for 30 seconds. The films were then dried at 120 °C for 30 min and the whole procedure was repeated few times to have desired number of coatings. The films were finally annealed at 500–700 °C (10 °C min^{-1}) for 4 h in air. The chemical microanalysis was performed on Ga_2O_3 and In_2O_3 films using energy dispersive X-ray spectroscopy (EDX), indicating the composition of the annealed films being Ga_2O_3 or In_2O_3. The films produced were further analysed by XRD and SEM measurements.

In contrast to the behaviour of Ga_2O_3 powder, X-ray diffraction patterns for the Ga_2O_3 films deposited on glass from **1** (single coating) and annealed at 500 °C for 4 h indicated that they were amorphous (Fig. S4).† These results are consistent with other reports where polycrystalline β-Ga_2O_3 films were obtained only after annealing the amorphous films above 700 °C.[16,21] The scanning electron microscopic (SEM) images of these Ga_2O_3 films showed a flat surface morphology with a thickness of 1 μm (Fig. 10 and ESI Fig. S5).† These films adhered very well to the glass substrate and passed the Scotch tape test. However, their adhesiveness was poor on Si wafer, which also precluded XRD of Ga_2O_3 films deposited on this substrate and annealed at 700 °C for 4 h. In contrast, the In_2O_3 films were better adhered on Si wafer surface. The crystalline nature of these films annealed at 700 °C was confirmed by X-ray powder diffraction. Fig. 11 shows the powder XRD of the film deposited from **2**, which is consistent with the reference standard for cubic In_2O_3 (JCPDS no. 006-0416). The film morphology was studied using SEM studies. Compared to the Ga_2O_3 film on glass (Fig. 10), surface of the In_2O_3 film was much rougher and large crystallites with well-defined grain boundaries were observed (Fig. 12, S6).† This is in good agreement with the typical trend of increased crystallite size upon raising the temperature. The films obtained after three coatings were approximately 0.5 μm thick, as determined by cross-sectional SEM measurements.

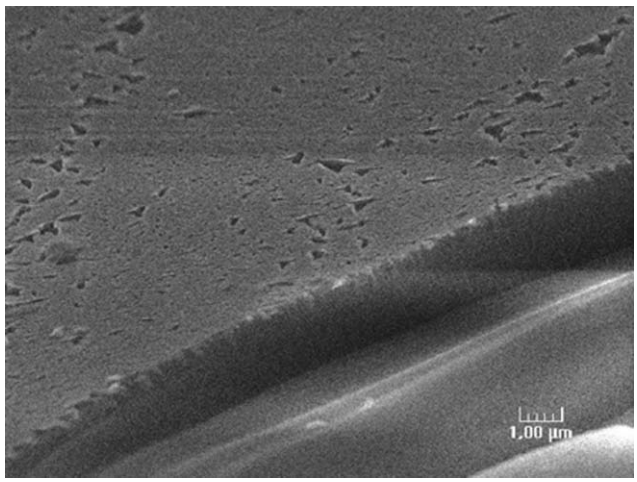

Fig. 10 SEM image of Ga_2O_3 film on glass slide obtained from **1**.

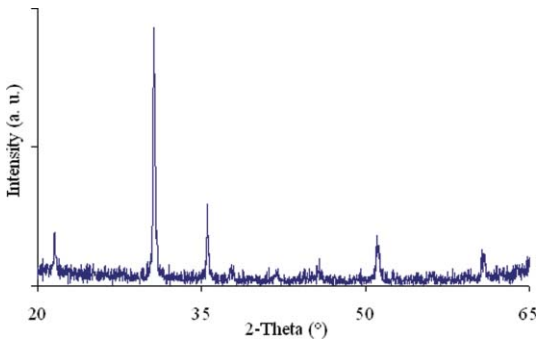

Fig. 11 XRD pattern of In_2O_3 film on Si wafer obtained from **2**.

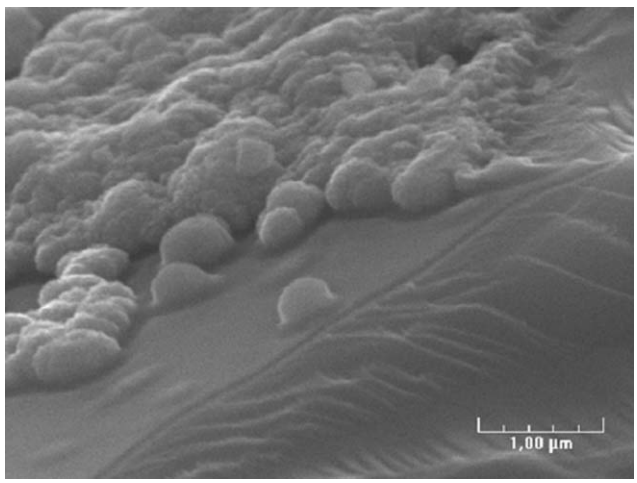

Fig. 12 SEM image of In_2O_3 film on Si wafer obtained from **2**.

Conclusion

New homoleptic aminoalkoxide derivatives of gallium(III) and indium(III) were prepared and characterised by elemental analysis, FT-IR and ^{1}H NMR spectroscopy as well as single-crystal X-ray analysis for $Ga_4\{\mu\text{-}\eta^3\text{:}\eta^1\text{-}(OC_2H_4)_2NMe\}_6$ (**1**·4$CHCl_3$) and $In_4\{\mu\text{-}\eta^3\text{:}\eta^1\text{-}(OC_2H_4)_2NMe\}_6$ (2·6$CHCl_3$). Hydrolyses of these compounds were investigated and the particle sizes were determined. Various sol-gel processing parameters were studied in order to

stabilise nanosized colloidal suspensions for access to thin films by spin coating. For comparison, similar studies were carried out for a previously known $Ga_2(dmea)_6$ and the parent gallium alkoxide $Ga(O^iPr)_3$. Irrespective of the type of gallium precursor selected, the hydrolysed powders showed similar pattern of phase transformation, from as-prepared Ga(O)OH to α-Ga_2O_3 at 500 °C and then β-Ga_2O_3 at 700 °C. The *N*-methyldiethanolamine derivatives **1** and **2** were found to be the most suitable candidates for sol–gel processing, allowing transparent and homogeneous M_2O_3 films to be deposited on glass or Si wafer, which were characterised by SEM, EDX and XRD measurements. The easy synthesis reported here makes these complexes valuable precursors for obtaining M_2O_3 nanomaterials. In case of gallium aminoalkoxides particularly, where *in situ* reaction of $Ga(O^iPr)_3$ and required aminoalcohol in suitable ratio can be followed by subsequent hydrolysis to obtain sol or gel directly, it is possible to avoid some synthetic steps such as isolation and purification of the precursors. Compared to precursors, the sols or gels obtained are more stable, easy to store, handle as well as fabricate in to homogeneous M_2O_3 materials.

Experimental

All manipulations were performed under argon atmosphere using Schlenk tube and vacuum line techniques. $GaCl_3$ and $InCl_3$ (both Aldrich) were used as received. Solvents were purified on an MB SPS-800 instrument and amino alcohols (Aldrich) were stored over molecular sieves. Gallium tris-isopropoxide was prepared as reported in the literature.[22] FT-IR spectra were recorded either as Nujol mulls (derivatives **1–3**, **A**) or KBr pellets (powders obtained after hydrolysis of precursors) on a Bruker Vector 22 spectrometer. ^{1}H NMR spectra were recorded on a Bruker AC-300 spectrometer. Analytical data were obtained from the Centre de Microanalyses du CNRS. TGA-DTA data of hydrolysed products were collected on a Setaram 92 system in air with a thermal ramp of 5 °C min^{-1}. Powder X-ray diffraction data were obtained with a Siemens D 5000 diffractometer using CuKα radiation. Particle sizes were measured in isopropanol solution with a Coulter N4 Plus submicron particle sizer. Cells were filled with isopropanol and 30–40 drops of the hydrolysed solutions (0.05–0.8 M) were added to achieve a scattering intensity of 5×10^4–1×10^6 counts s^{-1} at 90 °. SEM images were collected on Hitachi S800 spectrometers. The glass substrates and Si wafers were cleaned with acetone and dried at 120 °C prior to use.

Syntheses

$Ga_2(OC_2H_4NMe_2)_6$ (A). *N*, *N*-dimethylethanolamine (1.1 cm^3, 10.72 mmol) was added drop-wise to a toluene solution (10 cm^3) of $Ga(O^iPr)_3$ (0.88 g, 3.57 mmol) and the colourless solution obtained was stirred first at room temperature for 8 h and then under reflux for 2 h. Solvents were removed under vacuum to give a colourless viscous mass, which was crystallised from *n*-pentane at –20 °C as colourless solid. Yield, 0.77 g (65%). Anal. calcd for $C_{24}H_{60}N_6O_6Ga_2$: C 43.17, H 8.99, N 12.59. Found: C 43.0, H 9.01, N 12.62%. ν_{max} (Nujol)/cm^{-1}: 1749 w, 1621 w, 1582 w, 1269 m, 1087 m, 1032 m, 944 m, 900 m, 846 m, 777 m, 719 m, 630 m, 503 m (*ν*Ga–O and *ν*Ga–N). δ_H (300 MHz; $CDCl_3$) 3.86 (br, 12 H, OCH_2), 2.56 (br, 12 H, NCH_2), 2.32 (s, 36 H, NMe_2).

$Ga_4\{(OC_2H_4)_2NMe\}_6$ (1·4CHCl$_3$). Using the above procedure, **1** was obtained from $Ga(O^iPr)_3$ (0.69 g, 2.78 mmol) and *N*-methyldiethanolamine (0.48 cm^3, 4.18 mmol) in toluene and crystallised from chloroform at room temperature (0.78 g, 77%). Anal. calcd for $C_{30}H_{66}N_6O_{12}Ga_4{\cdot}4CHCl_3$: C 27.96, H 4.79, N 5.75. Found: C 27.76, H 4.75, N 5.78%. ν_{max} (Nujol)/cm^{-1}: 1288 m, 1263 m, 209 m, 1145 m, 1094 s, 1072 s, 1037 m, 993 s, 915 m, 895 s, 761 s, 723 s, 655 m, 596 m, 522 m, 488 m, 424 m (*ν*Ga–O and *ν*Ga–N). δ_H (300 MHz; $CDCl_3$) 7.25 (s, 4 H, $CHCl_3$), 3.72 (br, 24 H, OCH_2), 2.80 (br, 24 H, NCH_2), 2.50 (s, 18 H, NMe).

$In_4\{(OC_2H_4)_2NMe\}_6$ (2·6CHCl$_3$). To a THF suspension of Na_2mdea (prepared freshly by the reaction of NaH (0.70 g, 29.16 mmol) and $mdeaH_2$ (1.70 cm^3, 14.78 mmol) in 45 cm^3 THF under reflux for 1 h), a solution of $InCl_3$ (2.15 g, 9.72 mmol) in THF (40 cm^3) was added and the resulting reaction mixture was stirred first at room temperature for 24 h and then at 50 °C for 3 h. After cooling down the reaction mixture, all the THF was removed under vacuum and complex was extracted from chloroform (70 cm^3). After concentrating this solution up to 30 cm^3, crystals suitable for X-ray were obtained at room temperature by layering this chloroform solution with diethyl ether (30 cm^3). Yield, 3.10 g (68%). Anal. calcd for $C_{30}H_{66}N_6O_{12}In_4{\cdot}6CHCl_3$: C 22.99, H 3.51, N 4.47. Found: C 22.72, H 3.46, N 4.49%. ν_{max} (Nujol)/cm^{-1}: 1297 w, 1253 w, 1165 w, 1096 s, 1084 s, 1037 s, 1013 s, 929 w, 915 w, 898 s, 797 w, 753 w, 718 w, 640 m, 620 w, 601 w, 581 w, 558 m, 505 m, 454 m, 419 m (*ν*In–O and *ν*In–N). δ_H (300 MHz; $CDCl_3$) 7.25 (s, 6 H, $CHCl_3$), 3.80 (dt, J = 6.0 Hz, 24 H, OCH_2), 2.75 (dt, J = 6.0 Hz, 24 H, NCH_2), 2.48 (s, 18 H, NMe).

[Ga{$(OC_2H_4)_3N$}] (3). In a similar procedure described for **1**, the reaction of $Ga(O^iPr)_3$ (0.89 g, 3.62 mmol) and triethanolamine (0.49 ml, 3.64 mmol) in toluene gave **3** as colourless solid. After different crystallisation attempts to get X-ray quality crystals failed, this compound was washed twice with cold *n*-pentane (3 cm^3 each) to remove the slight excess of $teaH_3$. Yield, 0.69 g (89%). Anal. calcd for $C_6H_{12}NO_3Ga$: C 33.38, H 5.56, N 6.49. Found: C 33.43, H 5.58, N 6.51%. ν_{max} (Nujol)/cm^{-1}: 1271 m, 1160 w, 1096 s, 1073 s, 1013 s, 915 m, 892 s, 797 w, 718 w, 665 w, 596 m, 542 m, 459 w (*ν*Ga–O and *ν*Ga–N). δ_H (300 MHz; CD_3CN) 3.70 (br, 24 H, OCH_2), 2.75 (br, 24 H, NCH_2).

X-Ray crystallography of 1 and 2

Suitable crystals of **1** were grown from chloroform at room temperature as colourless plates and mounted on an Oxford XCALIBUR diffractometer. Cell parameters were refined using CrysAlis RED.[23] Absorption correction was applied with the Blessing Method.[24] The structure was solved using SHELXS97[25] and refined on F^2 by least squares using SHELXL-97.[26] All non-H atoms were refined anisotropically. Hydrogen atoms positions were calculated and refined but U_{iso} was fixed at 1.2 times that of the parent atom. Crystals of **2** were obtained from $CHCl_3$–Et_2O at room temperature and mounted on a Nonius Kappa CCD diffractometer. Intensities were collected by means of the COLLECT software.[27] Reflection indexing, Lorentz-polarisation correction, peak integration and background determination were carried out with DENZO.[28] Frame scaling and unit-cell parameters refinement were made with SCALEPACK.[28] An analytical absorption correction was applied using the modelled faces of the

Table 4 Crystallographic and refinement data of **1** and **2**

Compound	**1**	**2**
Empirical formula	$C_{30}H_{66}Ga_4N_6O_{12}.4CHCl_3$	$C_{30}H_{66}In_4N_6O_{12}.6CHCl_3$
Formula weight	1459.2	1878.47
Crystal system	Monoclinic	Triclinic
Space group	$C2/c$	$P\bar{1}$
a/Å	25.543(1)	11.3352(3)
b/Å	13.1025(3)	11.4351(3)
c/Å	21.012(1)	14.6085(4)
α/°	90	74.816(2)
β/°	124.017(7)	89.786(2)
γ/°	90	70.837(2)
V/Å^3	5828.7(6)	1719.14(8)
Z	4	1
μ/mm^{-1}	2.44	2.08
T/K	100	150
Measured reflections	41 086	15 429
Independent reflections (R_{int})	6700 (0.074)	8216 (0.031)
Data/restraints/parameters	6700/0/413	5411/0/370
GOF	1.00	1.13
R [$(F^2 > 2\sigma(F^2)$]	0.038	0.035
wR (F^2)	0.095	0.033
Residual electron density (e Å^{-3})	−0.97–1.16	−0.74–1.18

crystal.[29] The structure was solved by direct methods with SIR97.[30] The structure refinement was carried out with CRYSTALS.[31] Crystallographic and refinement data for **1** and **2** are given in Table 4.

Acknowledgements

S. M. is grateful to Centre National de la Recherche Scientifique (CNRS) for a post-doctoral fellowship. The help extended by S. Mangematin, M. Daniel (both IRCELYON) and Dr J.-M. Decams (ANNEALSYS) during the course of some experiments is also acknowledged.

References

1 (*a*) S.-Y. Lee, X. Gao and H. Matsui, *J. Am. Chem. Soc.*, 2007, **129**, 2954; (*b*) Y. Li, A. Trinchi, W. Wlodarski, K. Galatsis and K. Kalantar-Zadeh, *Sens. Actuators B*, 2003, **93**, 431; (*c*) M. Ogita, S. Yuasa, K. Kobayashi, Y. Yamada, Y. Nakanishi and Y. Hatanaka, *Appl. Surf. Sci.*, 2003, **212–213**, 397; (*d*) M. Ogita, K. Higo and Y. Hatanaka, *Appl. Surf. Sci.*, 2001, **175**, 721; (*e*) M. Fleischer and H. Mexiner, *Sens. Actuators B*, 1995, **26–27**, 81.

2 (*a*) D. P. Dutta, V. Sudarsan, P. Srinivasu, A. Vinu and A. K. Tyagi, *J. Phys. Chem. C*, 2008, **112**, 6781; (*b*) C.-H. Lee, M. Kim, T. Kim, A. Kim, J. Paek, J. W. Lee, S.-Y. Choi, K. Kim, J.-B. Park and K. Lee, *J. Am. Chem. Soc.*, 2006, **128**, 9326; (*c*) S. Sharma and M. K. Sunkara, *J. Am. Chem. Soc.*, 2002, **124**, 12288.

3 (*a*) R. Binions, C. J. Carmalt, I. P. Parkin, K. F. E. Pratt and G. A. Shaw, *Chem. Mater.*, 2004, **16**, 2489; (*b*) Y. Li, A. Trinchi, W. Wlodarski, K. Galatsis and K. Kalantar-Zadeh, *Sens. Actuators B*, 2003, **93**, 431; (*c*) M. Fleischer, S. Kornely, T. Weh, J. Frank and H. Meixner, *Sens. Actuators B*, 2000, **69**, 205; (*d*) M. Ogita, N. Saika, Y. Nakanishi and Y. Hatanaka, *Appl. Surf. Sci.*, 1999, **142**, 188.

4 (*a*) J. N. Avaritsiotis and R. P. Howson, *Thin Solid Films*, 1980, **80**, 63; (*b*) R. L. Weiher and R. P. Ley, *J. Appl. Phys.*, 1966, **37**, 299.

5 (*a*) G. C. Kim, J. S. Kim, E. S. Oh, J. C. Choi, K. Jeong, S. K. Chang, H. L. Park, T. W. Kim and C. D. Kim, *Mater. Res. Bull.*, 2000, **35**, 2409; (*b*) N. Naghavi, C. Marcel, L. Dupont, A. Rougier, J. B. Leriche and C. Guery, *J. Mater. Chem.*, 2000, **10**, 2315.

6 H. K. Muller, *Phys. Status Solidi B*, 1968, **27**, 723.

7 (*a*) T. Yuzhakova, V. Rakic, C. Guimon and A. Auroux, *Chem. Mater.*, 2007, **19**, 2970; (*b*) A. L. Petre, J. A. Peredigon-Melon, M. Hirano and H. Hosono, *Thin Solid Films*, 2002, **134**, 411; (*c*) A. L. Petre, A. Auroux, P. Gelin, M. Caldararu and N. I. Ionescu, *Thermochim. Acta*, 2001, **379**, 177; (*d*) C. O. Arean, A. L. Bellan, M. P. Menruit, M. R. Delagdo and G. T. Palomino, *Microporous Mesoporous Mater.*, 2000, **40**, 35.

8 (*a*) T. Miyata, T. Nakatkani and T. Minami, *Thin Solid Films*, 2000, **373**, 145; (*b*) J. Hao and M. Cocivera, *J. Phys. D: Appl. Phys.*, 2002, **35**, 433; (*c*) L. Binet and D. Gourier, *J. Phys. Chem. Solids*, 1998, **59**, 1241.

9 (*a*) S. Mishra, S. Daniele and L. G. Hubert-Pfalzgraf, *Chem. Soc. Rev.*, 2007, **36**, 1770; (*b*) L. G. Hubert-Pfalzgraf, *Inorg. Chem. Commun.*, 2003, **6**, 102; (*c*) L. G. Hubert-Pfalzgraf, *Appl. Organomet. Chem.*, 1998, **12**, 221; (*d*) L. G. Hubert-Pfalzgraf, *Coord. Chem. Rev.*, 1998, **178–180**, 967.

10 C. J. Brinker and G. W. Scherer, *Sol-gel Science: The Physics and Chemistry of Sol-gel processing*, Academic Press, San Diego, CA, 1990.

11 See for example: (*a*) J. Le Bris, L. G. Hubert-Pfalzgraf, S. Daniele and J. Vaissermann, *Inorg. Chem. Commun.*, 2007, **10**, 80; (*b*) R. W. Saalfrank, A. Scheurer, I. Bernt, F. W. Heinemann, A. V. Postnikov, V. Schunemann, A. X. Trautwein, M. S. Alam, H. Rupp and P. Muller, *Dalton Trans.*, 2006, 2865; (*c*) T. Kemmitt, L. G. Hubert-Pfalzgraf, G. J. Gainsford and R. Richard, *Inorg. Chem. Commun.*, 2005, **8**, 1149; (*d*) E. M. Rumberger, L. N. Zakharov, A. L. Rheingold and D. N. Hendrickson, *Inorg. Chem.*, 2004, **43**, 6531; (*e*) R. Matero, M. Ritala, M. Leskela, T. Sajavaara, A. C. Jones and J. L. Roberts, *Chem. Mater.*, 2004, **16**, 5630; (*f*) R. W. Saalfrank, C. Deutscher, S. Sperner, T. Nakajima, A. M. Ako, E. Uller, F. Hampel and F. W. Heinemann, *Inorg. Chem.*, 2004, **43**, 4372; (*g*) A. Singh and R. C. Mehrotra, *Coord. Chem. Rev.*, 2004, **248**, 101; (*h*) P. Werndrup, S. Gohil, V. G. Kessler, M. Kritikos and L. G. Hubert-Pfalzgraf, *Polyhedron*, 2001, **20**, 2163; (*i*) R. W. Saalfrank, I. Bernt, M. M. Chowdhry, F. Hampel and G. B. M. Vaughan, *Chem.–Eur. J.*, 2001, **7**, 2765; (*j*) Y. Chi, S. Ranjan, T.-Y. Chou, C.-S. Liu, S.-M. Peng and G.-H. Lee, *J. Chem. Soc., Dalton Trans.*, 2001, 2462.

12 C. J. Carmalt and S. J. King, *Coord. Chem. Rev.*, 2006, **250**, 682.

13 (*a*) A. Willner, A. Hepp and N. W. Mitzel, *Dalton Trans.*, 2008, 6832; (*b*) S. Basharat, C. E. Knapp, C. J. Carmalt, S. A. Barnett and D. A. Tocher, *New J. Chem.*, 2008, **32**, 1513; (*c*) H. Schumann, S. Dechert, F. Girgsdies, B. Heymer, M. Hummert, J.-Y. Hyeon, J. Kaufmann, S. Schutte, S. Wernik and B. C. Wassermann, *Z. Anorg. Allg. Chem.*, 2006, **632**, 251; (*d*) R. W. Saalfrank, C. Deutscher, H. Maid, A. M. Ako, S. Sperner, T. Nakajima, W. Bauer, F. Hampel, B. A. Heb, N. J. R. van Eikema Hommes, R. Puchta and F. W. Heinemann, *Chem.–Eur. J.*, 2004, **10**, 1899; (*e*) S. Daniele, D. Tcheboukov, L. G. Hubert-Pfalzgraf and S. Lecocq, *Inorg. Chem. Commun.*, 2002, **5**, 347; (*f*) K.-H. Thiele, E. Hecht, T. Gelbrich and U. Dumichen, *J. Organomet. Chem.*, 1997, **540**, 89; (*g*) S. J. Rettig, A. Storr and J. Trotter, *Can. J. Chem.*, 1974, **52**, 2206.

14 (*a*) S. Basharat, C. J. Carmalt, R. Binions, R. Palgrave and P. Parkin, *Dalton Trans.*, 2008, **591**; (*b*) S. Basharat, C. J. Carmalt, R. Palgrave, S. A. Barnett, D. A. Tocher and H. O. Davies, *J. Organomet. Chem.*, 2008, **693**, 1787; (*c*) S. Basharat, C. J. Carmalt, S. A. Barnett, D. A. Tocher and H. O. Davies, *Inorg. Chem.*, 2007, **46**, 9473; (*d*) Y. Chi, T.-Y. Chou, Y.-J. Wang, S.-F. Huang, A. J. Carty, L. Scoles, K. A. Udachin, S.-M. Peng and G.-H. Lee, *Organometallics*, 2004, **23**, 95; (*e*) S. Basharat, C. J. Carmalt, S. J. King, E. S. Peters and D. A. Tocher, *Dalton Trans.*, 2004, 3475; (*f*) T.-Y. Chou, Y. Chi, S.-F. Huang and C.-S. Liu, *Inorg. Chem.*, 2003, **42**, 6041.

15 (*a*) M. Yang, J. Yuan and P. Yue, *J. Sol-Gel Sci. Technol.*, 2008, **47**, 115; (*b*) N. B. H. Tahar, R. B. H. Tahar, A. B. Salah and A. Savall, *J. Am. Ceram. Soc.*, 2008, **91**, 846; (*c*) G. I. Spijksma, C. Huiskes, N. E. Benes, H. Kruidhof, D. H. A. Blank, V. G. Kessler and H. J. M. Bouwmeester, *Adv. Mater.*, 2006, **18**, 2165; (*d*) S. N. Koc, *J. Sol-Gel Sci. Technol.*, 2006, **38**, 277; (*e*) U. Aust, S. Benfer, M. Dietze, A. Rost and G. Tomandl, *J. Membr. Sci.*, 2006, **281**, 463; (*f*) S. Daniele, D. Tcheboukov and L. G. Hubert-Pfalzgraf, *J. Mater. Chem.*, 2002, 2519.

16 M. Valet and D. M. Hoffman, *Chem. Mater.*, 2001, **13**, 2135.

17 M.-A. Munoz-Hernandez, P. Wei, S. Liu and D. A. Atwood, *Coord. Chem. Rev.*, 2000, **210**, 1.

18 J. Pinkas and J. G. Verkade, *Inorg. Chem.*, 1993, **32**, 2711.

19 (*a*) A. C. Tas, P. J. Majewski and F. Aldinger, *J. Am. Chem. Soc.*, 2002, **85**, 1421; (*b*) M. Orita, H. Hiramatsu, H. Ohta, M. Hirano and H. Hosono, *Thin Solid Films*, 2002, **411**, 134.
20 (*a*) R. Rahal, S. Daniele, L. G. Hubert-Pfalzgraf, V. Guyot-Ferreol and J.-F. Tranchant, *Eur. J. Inorg. Chem.*, 2008, 980; (*b*) G. Goutailler, C. Guillard, S. Daniele and L. G. Hubert-Pfalzgraf, *J. Mater. Chem.*, 2003, **13**, 342.
21 (*a*) C. L. Dezelah, J. Niinisto, K. Arstila, L. Niinisto and C. H. Winter, *Chem. Mater.*, 2006, **18**, 471; (*b*) G. A. Battiston, R. Gerbasi, M. Porchia, R. Bertoncello and F. Caccavale, *Thin Solid Films*, 1996, **279**, 115.
22 R. C. Mehrotra and R. K. Mehrotra, *Curr. Sci.*, 1964, **33**, 241.
23 *CrysAlis CCD* and *CrysAlis RED*, ver. 1.171.26, Oxford Diffraction Ltd., Abingdon, UK, 2005.
24 R. H. Blessing, An empirical correction for absorption anisotropy, *Acta Crystallogr., Sect. A: Found. Crystallogr.*, 1995, **51**, 33.
25 G. M. Sheldrick, *SHELXS-97, Program for solution of crystal structures*, University of Göttingen, Germany, 1997.
26 G. M. Sheldrick, *SHELXL-97, Program for refinement of crystal structures*, University of Göttingen, Germany, 1997.
27 B. V. Nonius, *COLLECT*, Nonius, Delft, The Netherlands 1997–2001.
28 Z. Otwinowski and W. Minor, *Methods Enzymol.*, ed. C. W. Carter, Jr. and R. M. Sweet, Academic Press, New York, 1997, vol. 276, pp. 307.
29 J. de Meulenaar and H. Tompa, *Acta Crystallogr., Sect. A: Found. Crystallogr.*, 1965, **19**, 1014.
30 A. Altomare, M. C. Burla, M. Camalli, G. L. Cascarano, C. Giacovazzo, A. Guagliardi, A. G. G. Moliterni, G. Polidori and R. Spagna, *J. Appl. Crystallogr.*, 1999, **32**, 115.
31 D. J. Watkin, C. K. Prout and L. J. Pearce, *CAMERON*, Chemical Crystallography Laboratory, Oxford, UK, 1996.